SYSTEMS, SCIENCE AND SOFTWARE

SSS-R-76-2865

TELESEISMIC COUPLING FROM THE SIMULTANEOUS DETONATION OF AN ARRAY OF NUCLEAR EXPLOSIONS

J. T. Cherry
T. C. Bache
W. O. Wray
J. F. Masso

Topical Report

Sponsored by

Advanced Research Projects Agency
ARPA Order No. 2551

This research was supported by the Advanced Research Projects Agency of the Department of Defense and was monitored by AFTAC/VSC, Patrick AFB FL 32925, under Contract No. F08606-75-C-0045.

February 10, 1976

P. O. BOX 1620, LA JOLLA, CALIFORNIA 92038, TELEPHONE (714) 453-0060

SYSTEMS, SCIENCE AND SOFTWARE

SSS-R-76-2865

TELESEISMIC COUPLING FROM THE SIMULTANEOUS DETONATION OF AN ARRAY OF NUCLEAR EXPLOSIONS

J. T. Cherry
T. C. Bache
W. O. Wray
J. F. Masso

Topical Report

Sponsored by

Advanced Research Projects Agency
ARPA Order No. 2551

This research was supported by the Advanced Research Projects Agency of the Department of Defense and was monitored by AFTAC/VSC, Patrick AFB FL 32925, under Contract No. F08606-75-C-0045.

February 10, 1976

P. O. BOX 1620, LA JOLLA, CALIFORNIA 92038, TELEPHONE (714) 453-0060

UNCLASSIFIED

SECURITY CLASSIFICATION OF THIS PAGE (When Data Entered)

REPORT DOCUMENTATION PAGE		READ INSTRUCTIONS BEFORE COMPLETING FORM
1. REPORT NUMBER	2. GOVT ACCESSION NO.	3. RECIPIENT'S CATALOG NUMBER
4. TITLE (and Subtitle) TELESEISMIC COUPLING FROM THE SIMULTANEOUS DETONATION OF AN ARRAY OF NUCLEAR EXPLOSIONS,		5. TYPE OF REPORT & PERIOD COVERED Topical Report
		6. PERFORMING ORG. REPORT NUMBER SSS-R-76-2865
7. AUTHOR(s) J. T. Cherry, T. C. Bache, W. O. Wray and J. F. Masso		8. CONTRACT OR GRANT NUMBER(s) F08606-75-C-0045
9. PERFORMING ORGANIZATION NAME AND ADDRESS Systems, Science and Software P. O. Box 1620 La Jolla, California 92038		10. PROGRAM ELEMENT, PROJECT, TASK AREA & WORK UNIT NUMBERS Program Code No. 6F10 ARPA Order No. -2551
11. CONTROLLING OFFICE NAME AND ADDRESS VELA SEISMOLOGICAL CENTER 312 Montgomery Street Alexandria, Virginia 22314		12. REPORT DATE Feb[illegible] 1976
		13. NUMBER OF PAGES 26
14. MONITORING AGENCY NAME & ADDRESS (if different from Controlling Office) 12 32 p.		15. SECURITY CLASS. (of this report) Unclassified
		15a. DECLASSIFICATION/DOWNGRADING SCHEDULE

16. DISTRIBUTION STATEMENT (of this Report)

Approved for public release; distribution unlimited

17. DISTRIBUTION STATEMENT (of the abstract entered in Block 20, if different from Report)

18. SUPPLEMENTARY NOTES

19. KEY WORDS (Continue on reverse side if necessary and identify by block number)

Explosion Seismology
Multiple Explosions
Constitutive Modeling
Shock Interaction
Teleseismic Magnitudes
Earth Structure
Seismic Coupling

20. ABSTRACT (Continue on reverse side if necessary and identify by block number)

Calculations performed to date have produced no significant enhancement of teleseismic ground motion from a multiple shot array. This was true in spite of the fact that the near source fracture pattern from the array differed significantly from that produced by a spherically symmetric explosion source. Fairly large perturbations in the seismic radiation pattern did appear but at frequencies outside the teleseismic band. → next page

DD FORM 1 JAN 73 1473 EDITION OF 1 NOV 65 IS OBSOLETE

388 507

UNCLASSIFIED

SECURITY CLASSIFICATION OF THIS PAGE (When Data Entered)

cont.

Enhanced tension failure did occur in the multiple shot calculation. However, for this to seriously affect teleseismic ground motion it would require an explosive spacing, yield and material properties combination in which fracturing from the array is much greater than that produced by a single charge of equivalent yield.

An array in which the important parameters are optimized to significantly alter the teleseismic ground motion could probably be constructed. However, it is much more likely that anomalous observations of teleseismic ground motion from an explosive array are due to overburden effects and high (low) coupling material properties. If these factors fail to explain the anomaly, shock interaction calculations should be performed but should be based on a good estimate of material strength for the rock at the test site.

TABLE OF CONTENTS

I. INTRODUCTION

This report presents the results of a theoretical study undertaken to determine if teleseismic ground motion may be enhanced by the simultaneous detonation of a closely spaced array of nuclear explosions. The specific array analyzed consisted of three 15 kt explosions equally spaced 165 meters apart. The explosive array was assumed contained, i.e., coupling effects due to cratering were not included in the analysis.

For this specific explosive array and the material properties assumed for the near source rock environment we found no significant change in the teleseismic signature of the multiple shot array over that produced by a single explosive of equivalent yield. This was true in spite of the fact that the near source fracture pattern from the array differed substantially from that produced by a single explosion.

A general answer to the question of the effect of shock interaction on teleseismic ground motion is not available from our study. However, our results indicate that if anomalous teleseismic magnitudes are observed from a particular explosive array, then the explanation should first be sought in the material properties and the overburden pressure associated with the specific rock type and depth of burial.

It may be possible for shock interaction to contribute to anomalous teleseismic magnitudes for an explosive array. However, for this to occur tension fracturing for the array must be much greater than that from a single explosion of equivalent yield. Since material strength is the key parameter which determines the extent of fracturing, it is very important that a firm estimate of this parameter be available before attempting to evaluate the effect of the shock interaction.

II. NEAR SOURCE GROUND MOTION

Details of the techniques used to predict the teleseismic ground motion from an explosive array have been presented previously (Cherry, et al., 1975a; Bache, et al., 1975). Basically the technique requires that the divergence, $\nabla \cdot \vec{S}$, and curl, $\nabla \times \vec{S}$, of the displacement field be monitored over a spherical surface which is outside the nonlinear material response region. The time histories of $\nabla \cdot \vec{S}$ and $\nabla \times \vec{S}$ are then decomposed into a multipole expansion in spherical harmonics. This expansion provides an equivalent point source representation which may be used to quantitatively establish the seismic coupling of the array.

Figure 2.1 shows a sketch of the explosive array, the nonlinear region and the spherical surface over which $\nabla \cdot \vec{S}$ and $\nabla \times \vec{S}$ were monitored. The computational grid extended far enough beyond this surface so that external reflections would not obviate the free field assumption.

The tensile fracture pattern around two adjacent cavities is shown in Figures 2.2 through 2.5. Note the "presplitting" between the cavities and the alteration of the fracture pattern from that expected from a spherically symmetric explosive source. This last item is illustrated dramatically in Figure 2.6 which shows the distribution of fractures in the entire grid at 11.57 msec. The portion of the grid displayed in Figure 2.5 is a subset of that shown in Figure 2.6. The fracture pattern above and to the left of the outer source is that expected from a single explosive. The alteration of this fracture pattern is caused by interaction of the stress fields from adjacent explosives.

The extent of fracturing is controlled by the assumed material strength. For this calculation we assume that material strength (Y) was related to stress state ($\bar{P}$) by

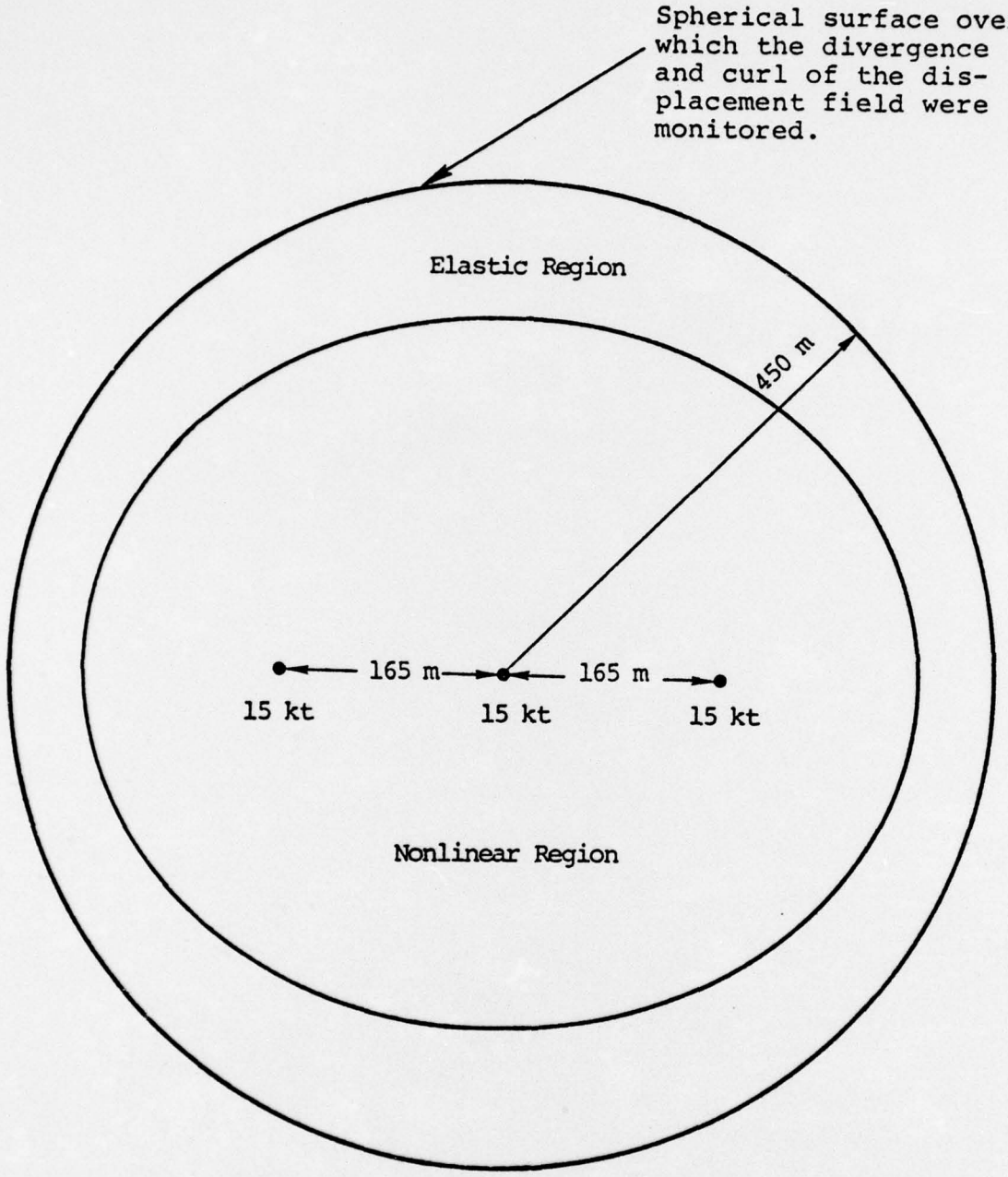

Figure 2.1. Sketch of the explosive array, the resulting nonlinear region and the surface over which the properties of the outgoing displacement field were monitored.

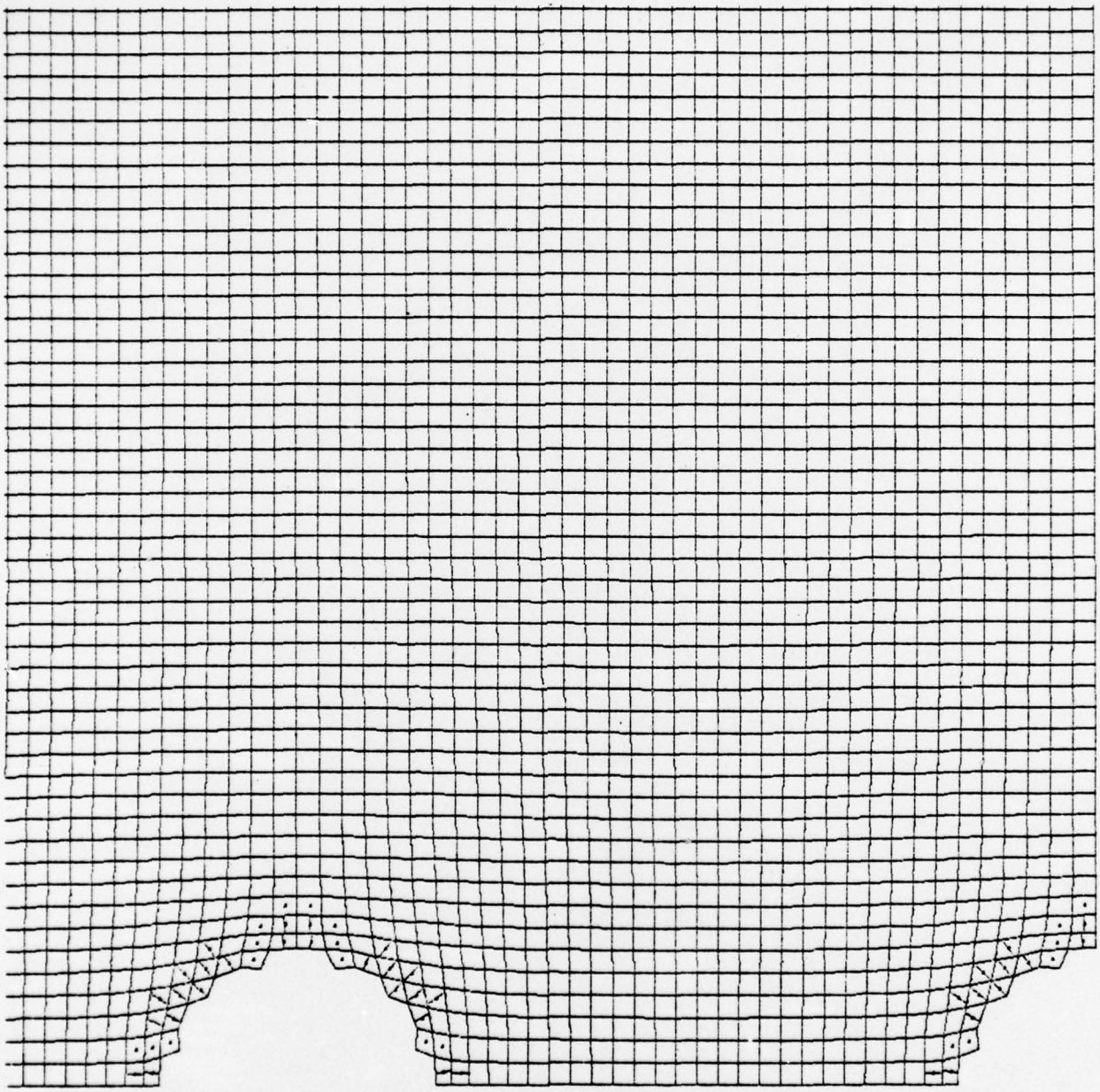

Figure 2.2. Crack location and orientation 4.93 msec after detonation. The lines indicate the crack orientation in the plane while a dot indicates a zone in which tensile failure out of the plane has occurred.

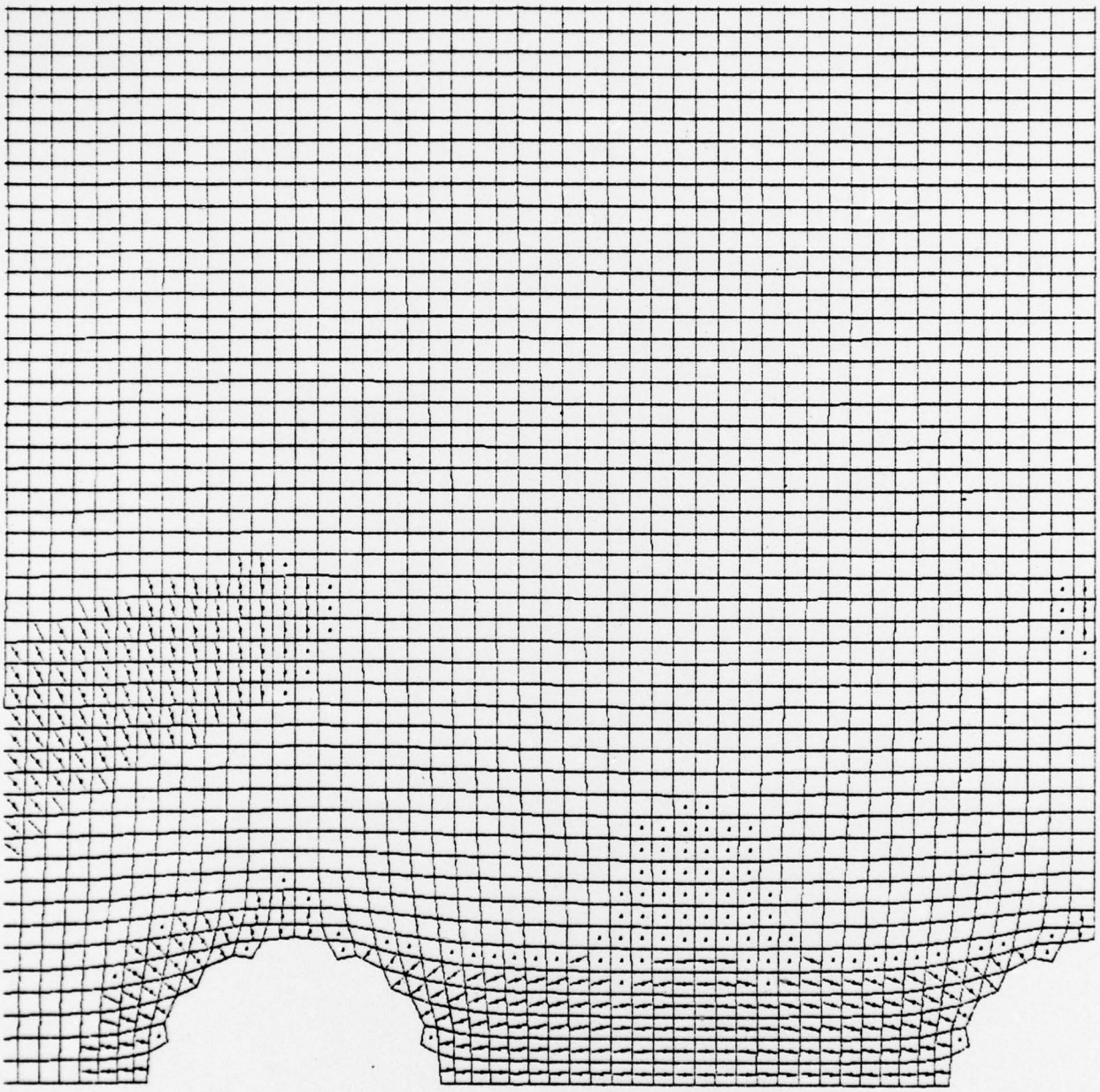

Figure 2.3. Crack location and orientation 6.85 msec after detonation.

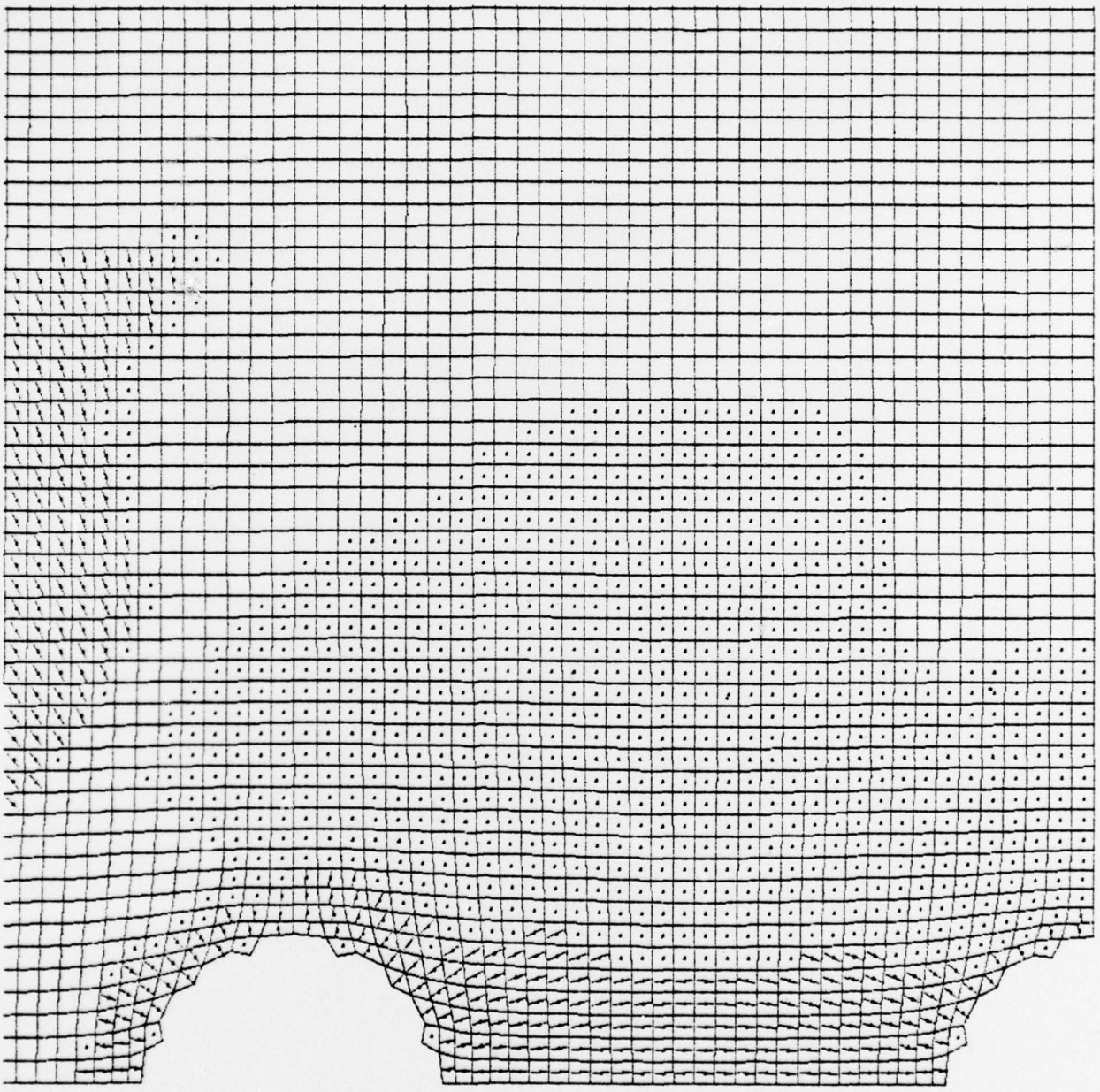

Figure 2.4. Crack location and orientation 9.21 msec after detonation.

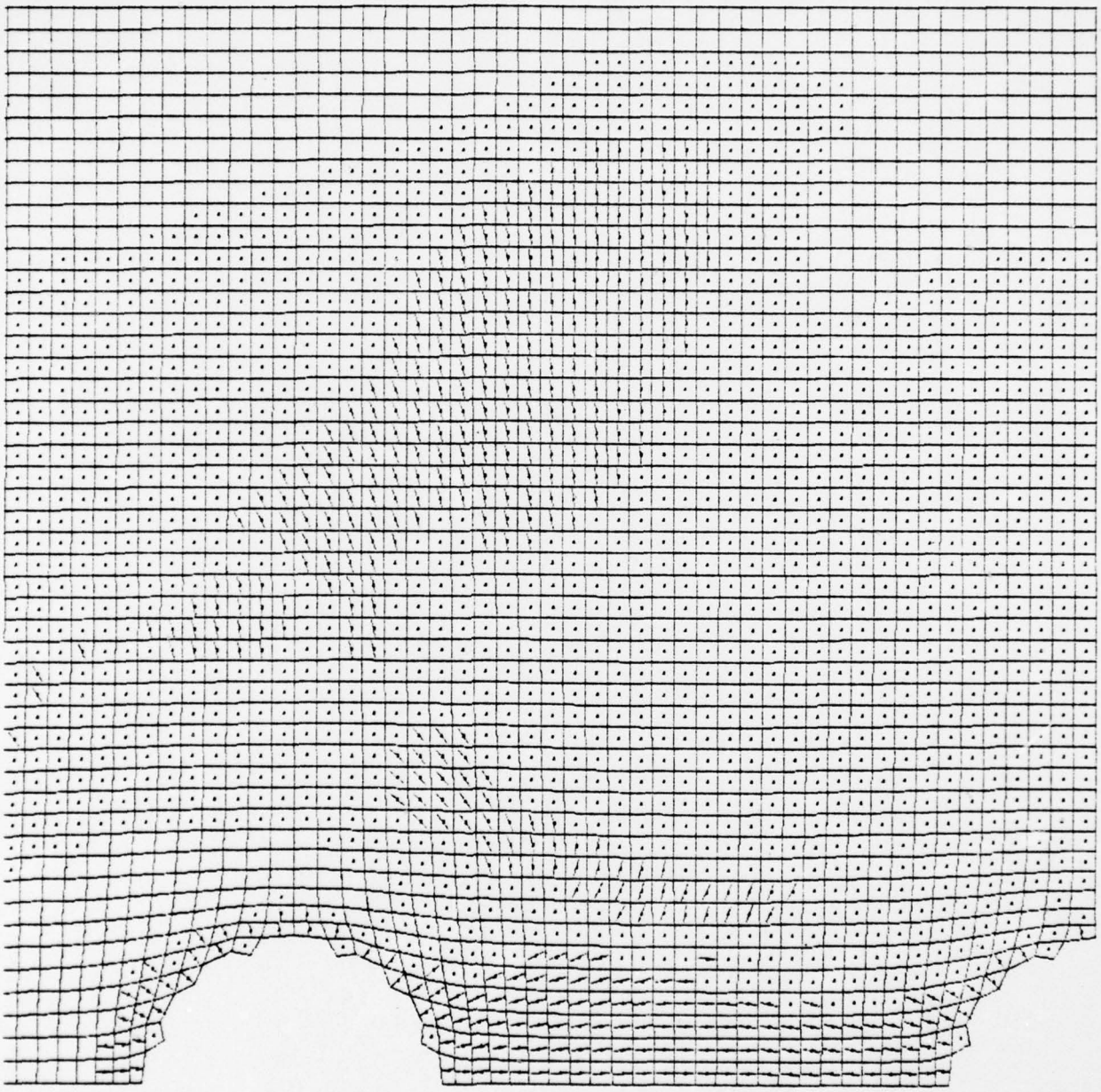

Figure 2.5. Crack location and orientation 11.57 msec after detonation.

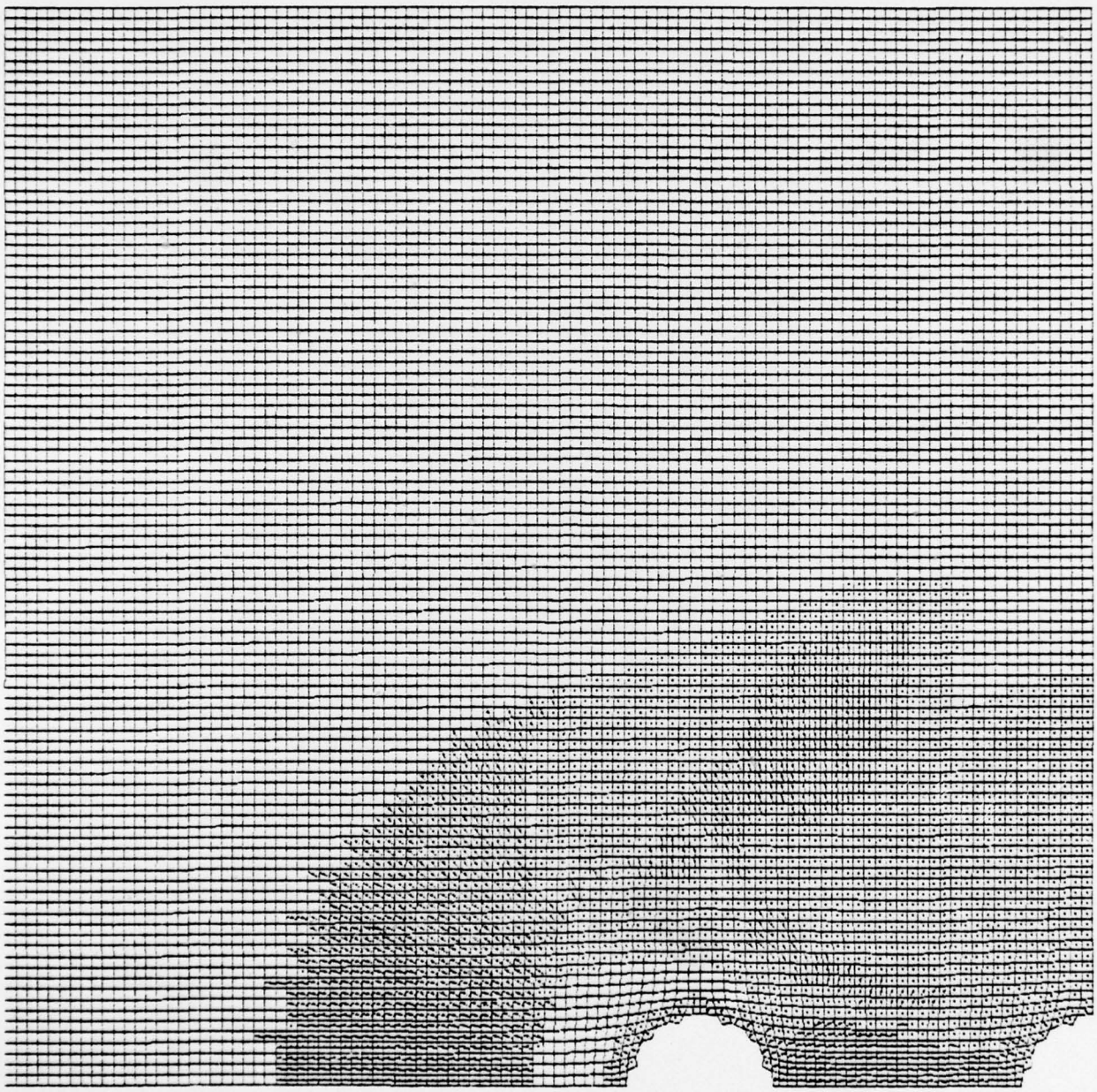

Figure 2.6. Complete crack location and orientation 11.57 msec after detonation.

$$Y = \left[Y_0 + Y_m \frac{\bar{P}}{\bar{P}_m} \left(2 - \frac{\bar{P}}{\bar{P}_m} \right) \right], \quad \bar{P} < P_m,$$

$$= Y_0 + Y_m, \qquad \bar{P} > P_m, \qquad (2.1)$$

$$= 0, \qquad Y < 0,$$

where

$$Y_0 = 0.4 \text{ kbar},$$

$$Y_m = 0.15 \text{ kbar},$$

$$\bar{P}_m = 0.45 \text{ kbar}.$$

The justification for assuming $Y = f(\bar{P})$ along with the tension failure model used when material strength is exceeded has been given by Cherry, et al. (1975b). For our purposes it will be sufficient to point out that a good measure of the tensile strength is given by $Y_0/2$; i.e., a tensile strength of 0.2 kbar was assumed for this calculation.

Our main objective was to determine if the fracture pattern unique to a multiple shot array could significantly effect teleseismic ground motion. The results shown in Figure 2.6 suggest that in the near field the multiple shot is quite different from a single explosion. In the next section it will be seen how these differences are transmitted to the far field. However, we must point out that the sensitivity of our results to tensile strength remains to be demonstrated.

Finally, we note that the maximum allowable stress difference assumed in this calculation was

$$Y_0 + Y_m = 0.55 \text{ kbar}.$$

This value is identical to that used for a previous calculation, reported by Cherry, et al. (1975c). However, no tension failure was allowed in the previous calculation. Taking the calculation described here together with the one reported by Cherry, et al. (1975c), we have two sources which will be described as the "no tensile failure" source and the "with tensile failure" source. In the first the multiple explosion array is different from a single explosion only in the asymmetry of the source arrangement. In the calculation described here, the effect of tensile failure is included.

In our previous report (Cherry, et al., 1975c) we showed that the "no tensile failure" multiple source calculation led to a teleseismic signature that was little different from that for a single explosion. In the following section the seismic radiation for both multiple sources will be discussed and compared to determine if teleseismic ground motion is significantly altered by the multiple shot array.

III. TELESEISMIC GROUND MOTION

In order to study the far field seismic signature of an explosion event like that considered here, it is necessary to merge the nonlinear finite difference source calculations presented in Section II with the elastic wave propagation methods of theoretical seismology. This is done via an equivalent elastic source representation of the multiple explosion source.

The familiar reduced displacement potential, RDP, representation of a spherically symmetric explosion is an elementary equivalent elastic source. For more complex sources a representation in terms of an expansion of the outgoing displacement field in spherical harmonics is appropriate. The calculation of an equivalent elastic source in this latter form for a complex asymmetric explosion source was first accomplished by Cherry, et al. (1975a). A detailed presentation of the theory and its implementation is given by Bache, et al. (1975). For convenience, a summary is given in Appendix A.

Using Eq. (A.5) of the appendix, an equivalent elastic source was computed for the multiple explosion source. The nonzero multipole coefficients included the monopole, $A_{00}^{(4)}(\omega)$, which is the spherically symmetric portion of the source. The nonzero higher order terms were

$$A_{\ell 0}^{(4)}(\omega),\ B_{\ell 1}^{(1)}(\omega) = -A_{\ell 1}^{(2)}(\omega),\ \ell = 2,\ 4,\ 6,\ \ldots\ ,$$

Where the 3-axis was taken to be along the line of explosion centers. The terms with $\ell = 2$ are referred to as the quadrupole terms and those with $\ell = 4$ as the octupole terms, etc.

The main objective is to determine the teleseismic signature of the multiple explosion. Therefore, it is

appropriate to draw conclusions from the far field portion of the displacement field; that is, only terms decaying with R^{-1} need be retained in the expansion, Eq. (A.5). In this case the P and S wave displacements reduce to

$$\bar{u}_p(R,\omega) = -\frac{e^{-ik_pR}}{k_p^2R}\left\{A_{00}^{(4)}(\omega) - A_{20}^{(4)}(\omega)\,\frac{(3\cos 2\theta+1)}{4} + \text{H.O.T.}\right\}$$

$$\bar{u}_s(R,\omega) = \frac{2e^{-ik_sR}}{k_s^2R}\left\{-\frac{3}{2}B_{21}^{(1)}(\omega)\sin 2\theta + \text{H.O.T.}\right\}, \qquad (3.1)$$

where H.O.T. indicates the higher order terms in the infinite series. In the frequency range of interest, terms higher than the quadrupole have almost no influence. The geometry is shown in Figure 3.1. With this geometry the displacements are independent of the "azimuthal" coordinate, ϕ.

The most direct way to study the equivalent elastic source is to examine the multipole coefficients themselves. The amplitude spectral density of the monopole and quadrupole coefficients is plotted in Figure 3.2. The coefficients for both source-calculations, with and without tension failure, are shown. From this plot the following is apparent:

- The monopole differences are mainly at short periods where the tensile failure model is larger (e.g., by a factor of 1.7 at 1 Hz).
- The P wave quadrupole ($A_{20}^{(4)}$) is an order of magnitude less than the monopole for frequencies less than 1 Hz for both sources. For higher frequencies the P wave quadrupole is increasingly more important. Selected ratios of $|A_{00}^{(4)}|$ to $|A_{20}^{(4)}|$ are as follows:

	With Tension Failure	No Tension Failure
2 Hz	1.8	4.3
3 Hz	0.7	2.0
4 Hz	0.6	1.2

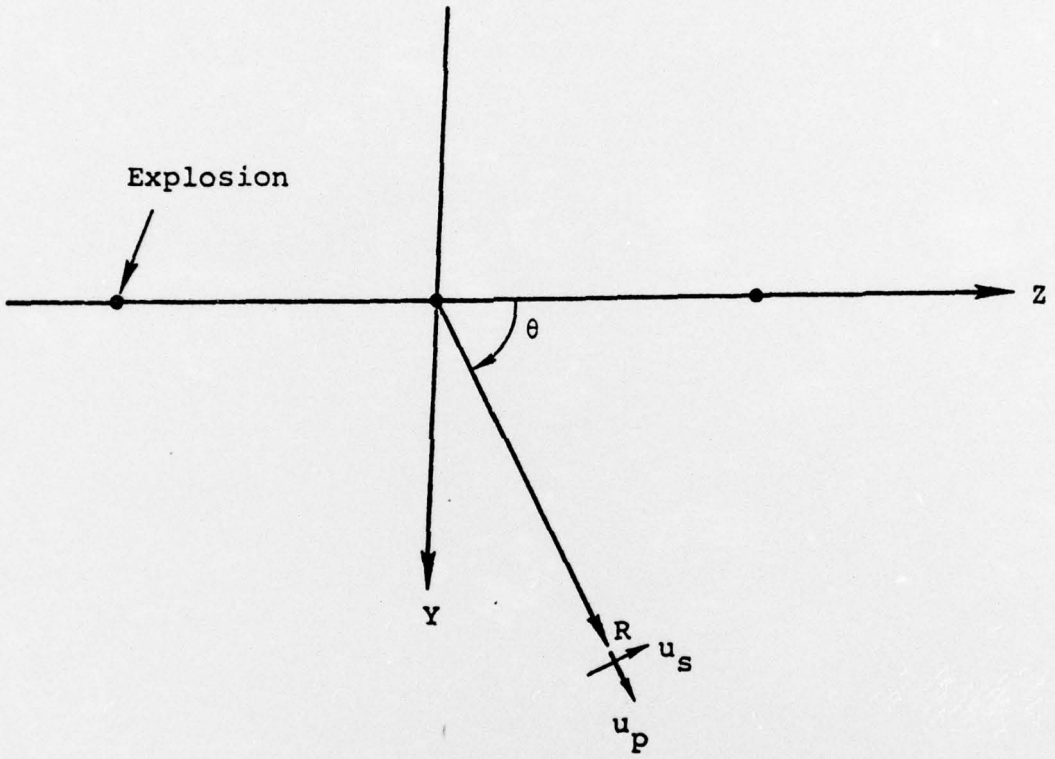

Figure 3.1. Geometry and coordinate system for the multiple explosion.

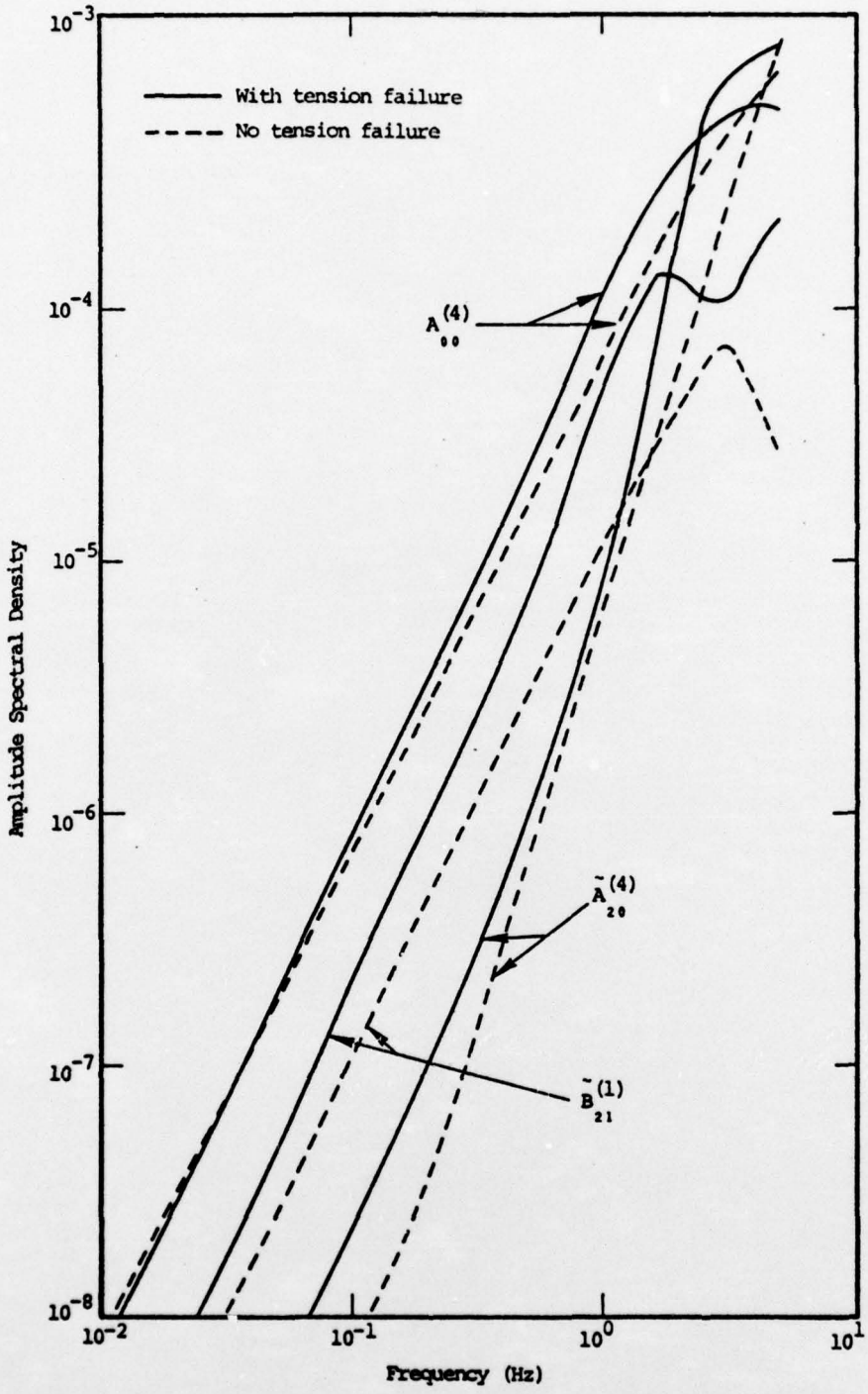

Figure 3.2. The amplitude spectral density of the multipole coefficients (monopole and quadrupole) for two multiple burst calculations, with and without tensile failure.

- The S wave quadrupole ($B_{21}^{(1)}$) is relatively constant with respect to the monopole. Selected ratios of $|A_{00}^{(4)}|$ to $|B_{21}^{(1)}|$ are tabulated below:

	With Tension Failure	No Tension Failure
0.05 Hz	3.8	6.8
0.5 Hz	3.1	6.2
1.0 Hz	2.4	5.8
2.0 Hz	2.7	6.3

From the tabulated values presented it is clear that tension failure does enhance the quadrupole perturbation on the spherically symmetric portion of the source. The enhancement is by a factor of two or so. However, except at high frequencies, the quadrupole terms remain too small to have much effect on the teleseismic signal.

A number of radiation patterns for the two sources are shown in Figures 3.3 and 3.4. The displacement spectral components in these patterns are normalized to those due to the monopole alone. The higher order perturbation on the spherically symmetric source is thereby directly displayed and is independent of R.

Examining the radiation patterns in Figure 3.3, it is clear that the "no tensile failure" source behaves, in terms of the far field radiation, almost the same as a spherically symmetric source. As was seen from the multipole coefficients, the addition of tensile failure increases the quadrupole component but it is still quite small (Figure 3.4). Even at 2 Hz the radiated P wave for the "with tensile failure" source is no more than 15 percent different from that due to the monopole alone. The S waves are, of course, much too small to contribute a significant sP phase to the early arriving body wave recording from which m_b measurements are made. However, it is true that rather large (for an explosion) direct S waves would be transmitted to the teleseismic field.

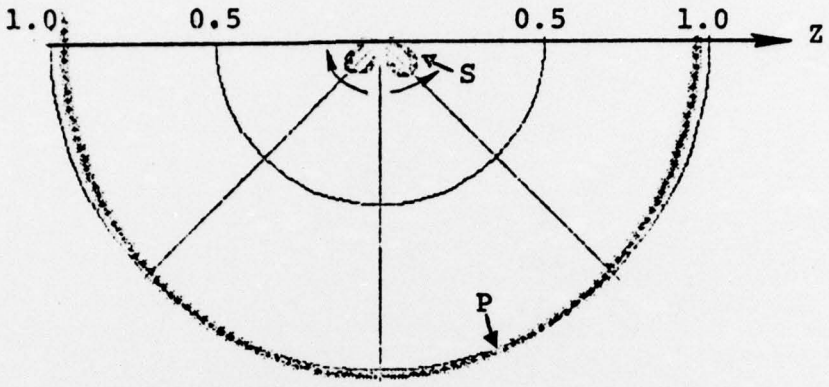

(a) 0.5 Hz

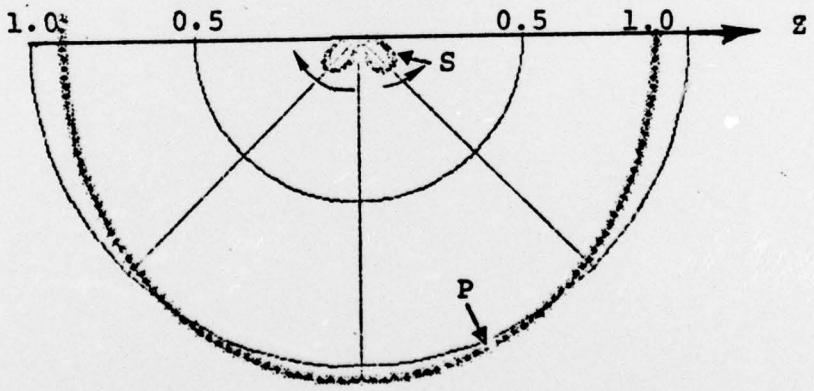

(b) 1.0 Hz

Figure 3.3. Radiation patterns for the "no tensile failure" multiple source calculation. These patterns show the far field P and S wave displacement spectral components normalized to that from the monopole contribution above. While included in the calculation, terms higher than the quadrupole make almost no contribution at these frequencies. These patterns are symmetric about the line of explosions which is indicated as the z-axis.

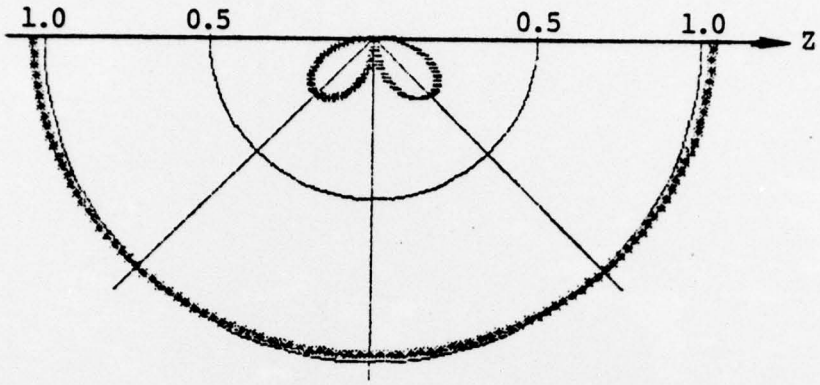

(a) 0.5 Hz

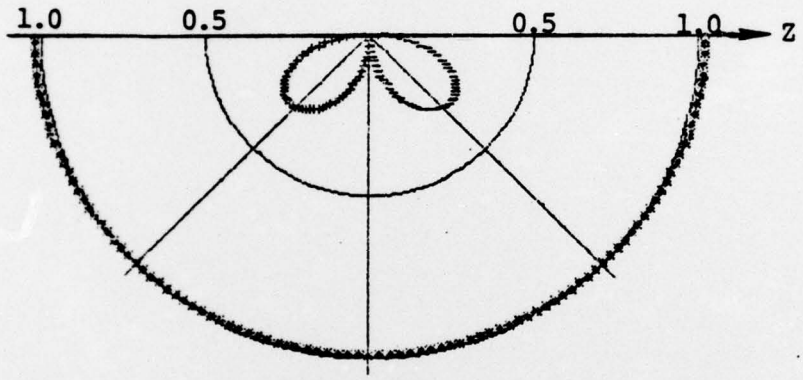

(b) 1.0 Hz

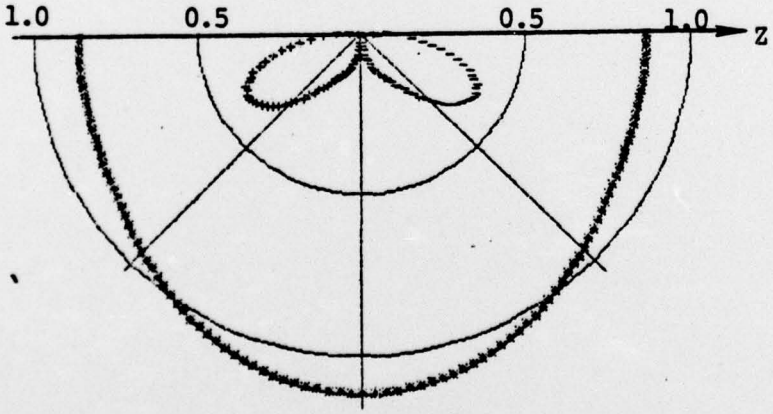

(c) 2.0 Hz

Figure 3.4. Radiation patterns like those of Figure 3.3 for the "with tensile failure" multiple source calculation.

From these radiation patterns and, as a double check, from a number of synthetic seismogram calculations, it was concluded that the multiple source appears, as far as teleseismic P wave and Rayleigh wave recordings are concerned, like a single spherically symmetric explosion. The only remaining question regards the yield of this equivalent single source. This can be determined by computing the RDP from the monopole using Eq. (A.8) of Appendix A. The "equivalent RDP" for the multiple explosion can then be compared to that obtained by a linear superposition of three single sources. RDP calculations for the tension failure and no tension failure cases are shown in Figure 3.5. The tension failure RDP shows the "overshoot" reported by Cherry, et al. (1975b).

In Figure 3.6 and 3.7 the amplitude of the transformed reduced velocity potential, $|\hat{\Psi}(\omega)|$, from the 1-D calculations (Figure 3.5) is compared to the equivalent quantity for the two multiple explosions under study. The linear superposition is done by (1) scaling the source as if it were a single 45 kt explosion and (2) considering the event to be the superposition of three 15 kt explosions. Due to the cube root scaling laws, the only difference in the two is that the second representation is somewhat richer in high frequencies.

From Figures 3.6 and 3.7, we see that for neither case does the "equivalent RDP" from the spherically symmetric portion of the multiple explosion calculation differ substantially from that obtained by a linear superposition of one-dimensional sources. It is interesting to note that the corner frequency for the no tensile failure calculation falls between that for the 3 × 15 kt and 45 kt superposition sources. For the second calculation, with tensile failure, the "equivalent RDP" is very little different than that for the 45 kt source.

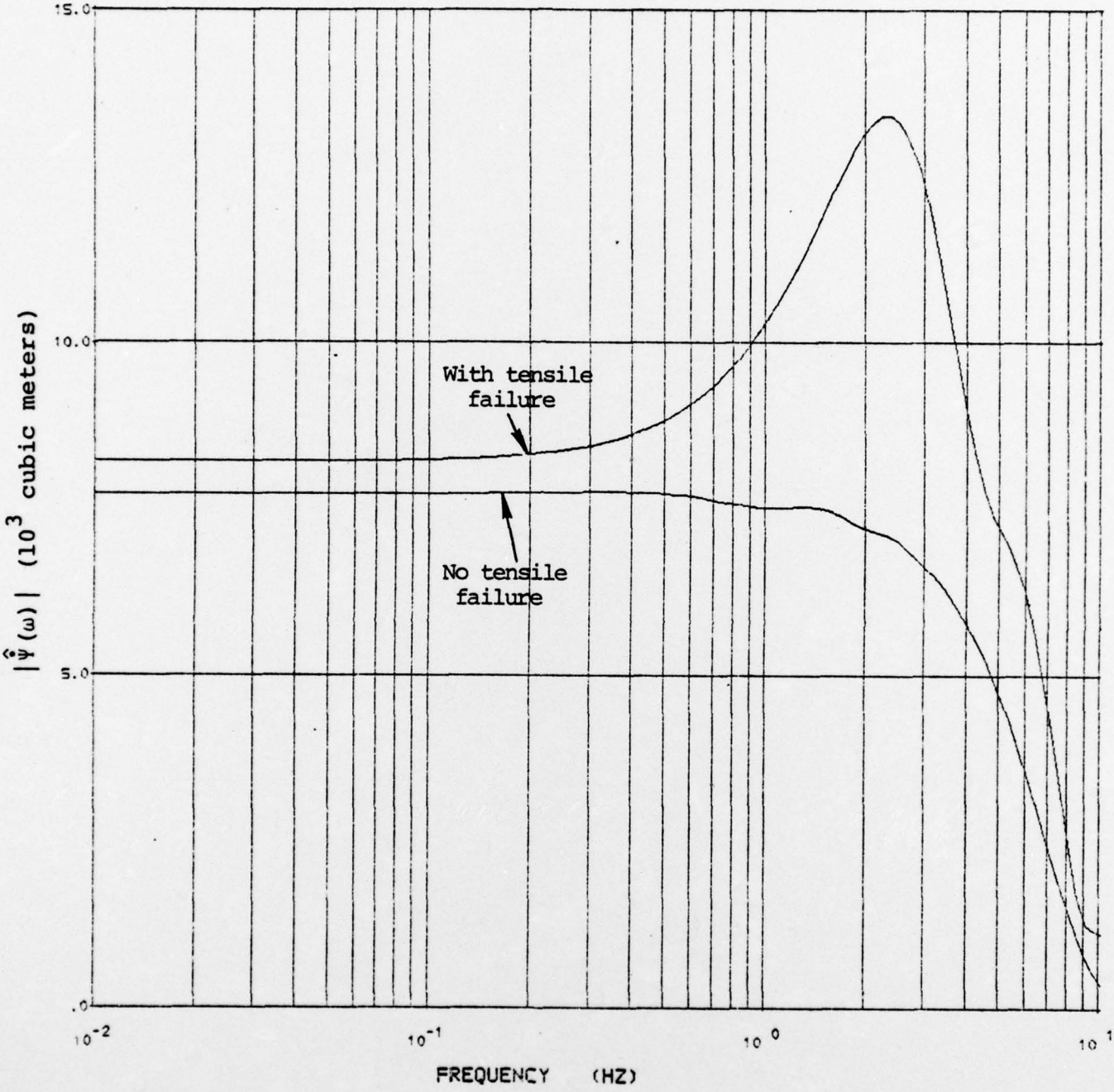

Figure 3.5. The amplitude of the transformed reduced velocity potential for two spherically symmetric explosion calculations. The explosion yield is 15 kt.

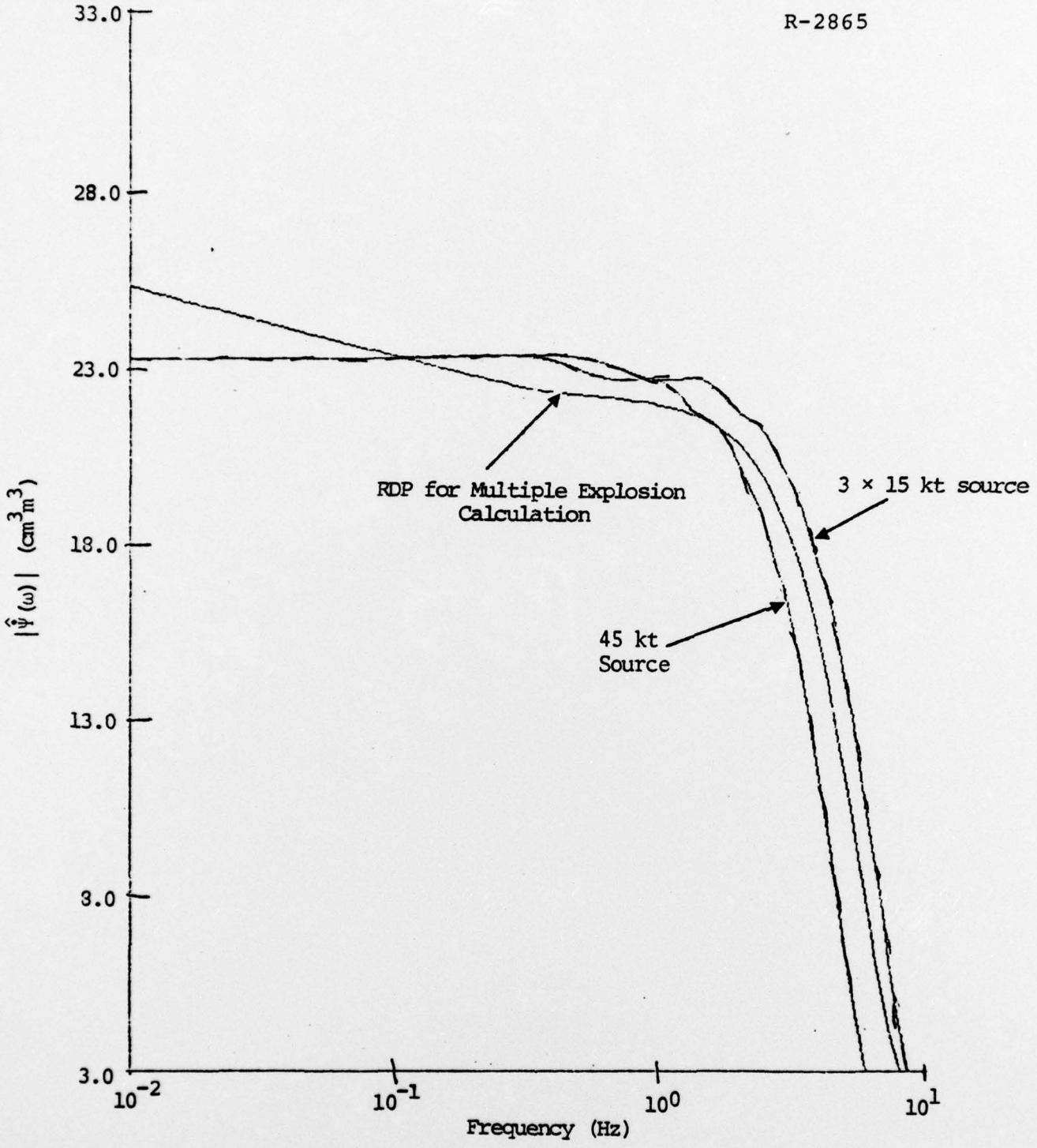

Figure 3.6. For the no tensile failure calculation, the "equivalent RDP" representation of the multiple shot is compared to the source obtained by a linear superposition of spherically symmetric explosions.

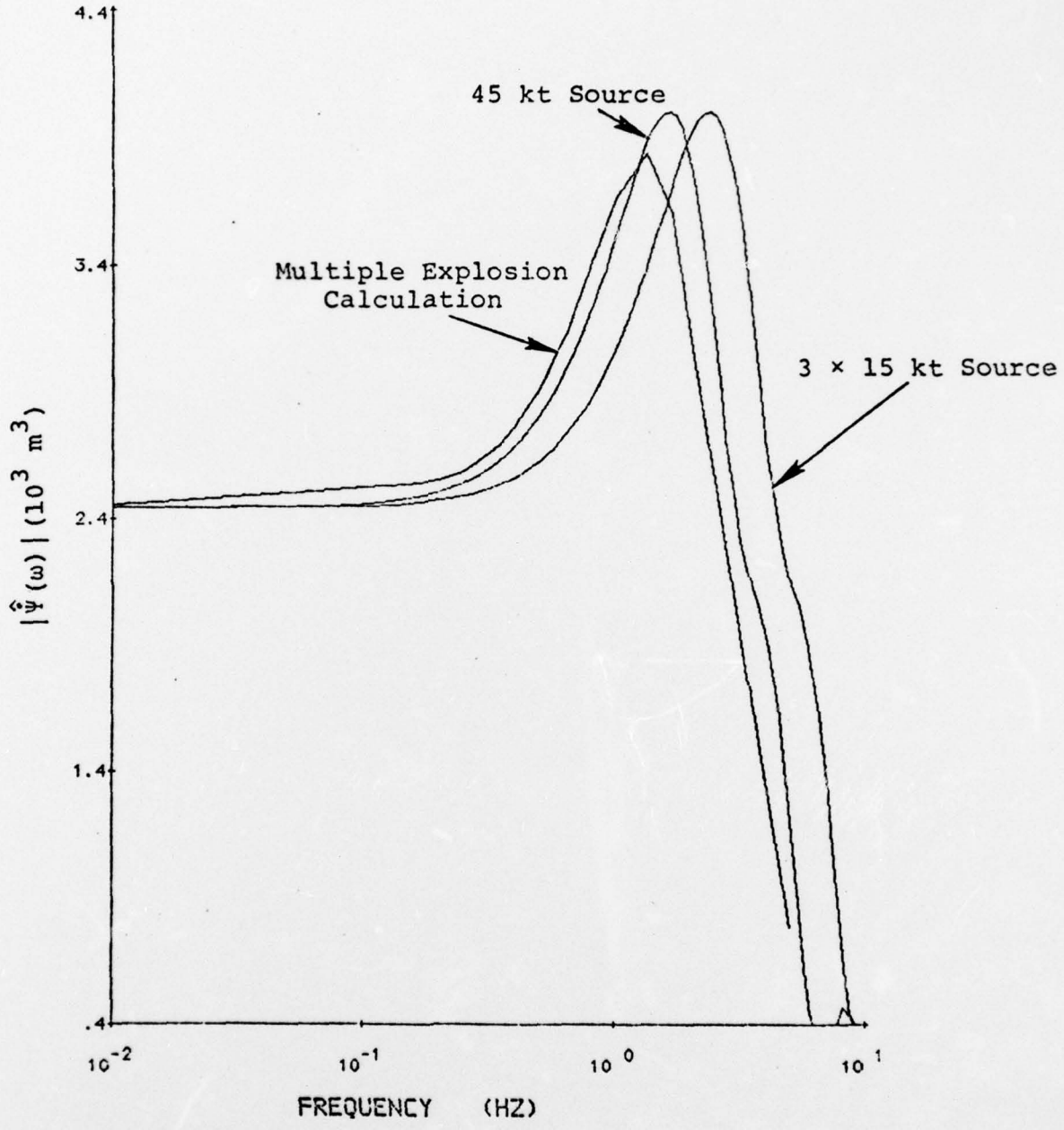

Figure 3.7. Comparison of the "equivalent RDP" representations of the multiple explosion for the calculations including the effect of tensile failure.

IV. SUMMARY AND CONCLUSIONS

Calculations performed to date have produced no significant enhancement of teleseismic ground motion from a multiple shot array. This was true in spite of the fact that the near source fracture pattern from the array differed significantly from that produced by a spherically symmetric explosion source. Fairly large perturbations in the seismic radiation pattern did appear but at frequencies outside the teleseismic band.

Enhanced tension failure did occur in the multiple shot calculation. However, for this to seriously affect teleseismic ground motion it would require an explosive spacing, yield and material properties combination in which fracturing from the array is much greater than that produced by a single charge of equivalent yield.

An array in which the important parameters are optimized to significantly alter the teleseismic ground motion could probably be constructed. However, it is much more likely that anomalous observations of teleseismic ground motion from an explosive array are due to overburden effects and high (low) coupling material properties. If these factors fail to explain the anomaly, shock interaction calculations should be performed but should be based on a good estimate of material strength for the rock at the test site.

APPENDIX A

EQUIVALENT ELASTIC SOURCE REPRESENTATION

The Fourier transformed equations of motion in a homogeneous, isotropic, linearly elastic medium may be written

$$\underset{\sim}{\bar{u}} = -\left(\frac{1}{k_\alpha^2}\right)\nabla\bar{\chi}^{(4)} + \left(\frac{2}{k_\beta^2}\right)\nabla \times \underset{\sim}{\bar{\chi}} \tag{A.1}$$

where $\underset{\sim}{\bar{u}}$ is particle displacement and k_α and k_β are the compressional and shear wave numbers. The Cartesian potentials $\bar{\chi}^{(4)}$ and $\underset{\sim}{\bar{\chi}}$ are defined by

$$\begin{aligned} \bar{\chi}^{(4)} &= \nabla \cdot \underset{\sim}{\bar{u}} \\ \underset{\sim}{\bar{\chi}} &= \frac{1}{2}\nabla \times \underset{\sim}{\bar{u}} \end{aligned} \tag{A.2}$$

and may be easily shown to satisfy the wave equation

$$\nabla^2\bar{\chi}^{(j)} + k_i^2\bar{\chi}^{(j)} = 0 \ , \ j = 1, 2, 3, 4, \tag{A.3}$$

where $k_4 \equiv k_\alpha = \omega/\alpha$, $k_i \equiv k_\beta = \omega/\beta$, $i = 1,2,3$. This equation has as a solution the following expansion in spherical eigenfunctions (e.g., Morse and Feshbach (1953)),

$$\bar{\chi}^{(j)}(\underset{\sim}{R},\omega) = \sum_{\ell=0}^{\infty} h_\ell^{(2)}(k_\alpha R) \sum_{m=0}^{\ell} \left[A_{\ell m}^{(j)}(\omega) \cos m\phi + B_{\ell m}^{(j)}(\omega) \sin m\phi\right] P_\ell^m(\cos\theta) \tag{A.4}$$

where the $h_\ell^{(2)}$ are spherical Hankel functions of the second kind and the P_ℓ^m are associated Legendre functions. The vector $\underset{\sim}{R}$ has as components the spherical coordinates R,θ,ϕ.

Equations (A.4) together with (A.1) provide an equivalent elastic source representation of the outgoing elastic

waves. The values of the multipole coefficients $A_{\ell m}^{(j)}(\omega)$, $B_{\ell m}^{(j)}(\omega)$, $j = 1,2,3,4$, prescribe the displacement field at all points in the homogeneous elastic medium where (A.1) applies.

The point source representation, Eq. (A.4), provides a generalization of the commonly used center of dilatation ($\ell = 0$), couple ($\ell = 1$) and double couple ($\ell = 2$) point sources, as well as more complex sources. For example, for a horizontal double couple source of unit amplitude, the non-zero coefficients in (A.4) are

$$-A_{21}^{(1)} = B_{21}^{(2)} = A_{22}^{(3)} = (\beta^2/\alpha^2)\, B_{22}^{(4)} .$$

Given the displacement, $\bar{u}_i$, or, alternatively, the potentials $\bar{\chi}^{(j)}$, one may determine the multipole coefficients using (A.4). For example, using the orthogonality of the spherical eigenfunctions, one may derive

$$\begin{Bmatrix} A_{\ell m}^{(j)}(\omega) \\ B_{\ell m}^{(j)}(\omega) \end{Bmatrix} = \frac{C_{\ell m}}{h_\ell^{(2)}(k_\alpha \hat{R})} \int_0^{2\pi} \int_0^{\pi} \bar{\chi}^{(j)}(\hat{R},\omega)\, P_\ell^m(\cos\theta) \begin{Bmatrix} \cos m\phi \\ \sin m\phi \end{Bmatrix} \sin\theta d\theta d\phi \qquad (A.5)$$

where

$$C_{\ell m} = \frac{(2\ell+1)(\ell-m)!}{2\pi(\ell+m)} , \quad m \neq 0 ,$$

$$C_{\ell_0} = (2\ell+1)/4\pi .$$

That is, given the displacements, $\bar{u}(\underset{\sim}{\hat{R}},\omega)$ on a sphere of radius $\hat{R}$, one can use (A.2), (A.5) and (A.4) to compute the displacements at any point in the elastic regime. This procedure was first suggested for geophysical applications by Archambeau (1968).

Using the equivalent elastic source representation, highly nonlinear finite difference calculations of the near

source earthquake or explosion displacement fields may be coupled to the elastic field where efficient elastic wave propagation techniques can be applied. Carrying the nonlinear computation out to a radius at which the material response is in the elastic regime, Eq. (A.5) may be applied to compute the multipole coefficients and, thereby, the equivalent elastic source.

For a spherically symmetric explosion, the explosion induced elastic field is often represented by the reduced displacement potential, $\psi(\tau)$, defined by

$$u_r(r,t) = \frac{\Psi(\tau)}{R^2} + \frac{1}{R_\alpha}\frac{d\Psi(\tau)}{d\tau} \quad , \tag{A.6}$$

where $\tau = t - R/\alpha$, is the retarded time. Note that $\Psi(\tau)$ is independent of R.

Applying the Fourier transform, (A.6) becomes

$$\bar{u}_r(R,\omega) = \frac{(1 + ik_\alpha r)}{R^2} e^{-ik_\alpha R} \bar{\Psi}(\omega) \quad . \tag{A.7}$$

Then, carrying out the algebra (observing that the $\bar{\underset{\sim}{u}}$ of (A.2) is the Cartesian displacement vector), it may be shown that the multipole coefficients reduce to a single nonzero term, the monopole:

$$A_{00}^{(4)}(\omega) = -ik_p^3 \bar{\Psi}(\omega) \quad . \tag{A.8}$$

REFERENCES

Archambeau, C. B., "General Theory of Elastodynamic Source Fields," Rev. Geophys., 6, pp. 241-288, 1968.

Bache, T. C., J. T. Cherry, K. G. Hamilton, J. F. Masso, and J. M. Savino, "Application of Advanced Methods for Identification and Detection of Nuclear Explosions from the Asian Continent," Systems, Science and Software Report SSS-R-75-2646, 1975.

Cherry, J. T., T. C. Bache and D. F. Patch, "The Teleseismic Ground Motion Generated by a Nuclear Explosion in a Tunnel and its Effects on the M_s/m_b Discriminant," Systems, Science and Software Final Contract Report, DNA 3645F, 1975a.

Cherry, J. T., N. Rimer, and W. O. Wray, "Seismic Coupling from a Nuclear Explosion: The Dependence of the Reduced Displacement Potential on the Nonlinear Behavior of the Near Source Rock Environment," Systems, Science and Software Report SSS-R-76-2742, 1975b.

Cherry, J. T., T. C. Bache and W. O. Wray, "Teleseismic Ground Motion from Multiple Underground Nuclear Explosions," Systems, Science and Software Report SSS-R-75-2709, 1975c.

Morse, P. M. and H. Feshbach, Methods of Theoretical Physics, McGraw-Hill, New York, 1953.